Arabian Journal of Chemistry (2022) **15**, 103592

King Saud University

Arabian Journal of Chemistry

www.ksu.edu.sa
www.sciencedirect.com

ORIGINAL ARTICLE

Synthesized Chitosan-Sodium Alginate-Polyethylene glycol-D-Pinitol nanocomposites showed antiarthritic activity on Freund's Complete Adjuvant-induced arthritis in rats

Shenqiang Qiu [a,*,1], Arunachalam Chinnathambi [b,1], Saleh H. Salmen [b], D.S. Prabakaran [c], Sulaiman Ali Alharbi [b], Vishnu Priya Veeraraghavan [e], Krishna Mohan Surapaneni [d]

[a] *Department of Hand and Foot Surgery, Shandong Provincial Hospital affiliated to Shandong First Medical University, No.324, Jingwu Road, Jinan, Shandong Province 250021, China*
[b] *Department of Botany and Microbiology, College of Science, King Saud University, PO Box -2455, Riyadh 11451, Saudi Arabia*
[c] *Department of Radiation Oncology, Chungbuk National University, College of Medicine, Cheongju 28644, Republic of Korea*
[d] *Department of Biochemistry, Panimalar Medical College Hospital & Research Institute, Varadharajapuram, Poonamallee, Chennai 600 123, India*
[e] *Department of Biochemistry, Saveetha Dental College, Saveetha Institute of Medical and Technical Sciences, Saveetha University, Chennai 600 077, India*

Received 19 October 2021; accepted 23 November 2021
Available online 27 November 2021

KEYWORDS

Arthritis;
Nanomedicine;
Lymphocytes;
D-Pinitol;
Chitosan;
Interleukin-1β;
Joint deformity

Abstract *Background:* Osteoarthritis is a severe degenerative joint disease characterized by swelling, joint pain, degradation of cartilage extracellular matrix, synovitis, callus formation, and loss of normal joint movements, which leads to functional limitations and seriously affect the patient's life quality.

Objective: The current research work was focussed to synthesize and characterize the chitosan-sodium alginate-polyethylene glycol-d-pinitol nanocomposites (CSP-dP-NCs) and evaluate its anti-arthritic activity against the freund's complete adjuvant (FCA)-triggered arthritis in animals.

Methodology: The CSP-dP-NCs were synthesized by standard method. The development and properties of formulated CSP-dP-NCs were confirmed by several characterization techniques like

* Corresponding author.at: Department of Hand and Foot Surgery, Shandong Provincial Hospital affiliated to Shandong First Medical University, No.324, Jingwu Road, Jinan, Shandong Province 250021, China.
E-mail address: qiusq2569@163.com (S. Qiu).
[1] Equal contribution.

Peer review under responsibility of King Saud University.

Production and hosting by Elsevier

https://doi.org/10.1016/j.arabjc.2021.103592

UV–visible, photoluminescence, X-ray diffractometer (XRD), Fourier Transform-Infrared (FT-IR), scanning electron microscopic (SEM), energy dispersive X-ray (EDX), and dynamic light scattering (DLS) analyses. The arthritis was induced in experimental rats via administering 0.1 ml of FCA subcutaneously and then treated with 10 and 25 mg/kg of synthesized CSP-dP-NCs for 25 days. The bodyweight of animals were tabulated and then haematological parameters, organ index, and paw volume was examined. The levels of liver marker enzymes were assessed by standard techniques. The contents and pro-inflammatory cytokines and antioxidant parameters were quantified using assay kits.

Results: The findings of characterization studies confirmed the development of CSP-dP-NCs with size ranging from 180 nm, tetragonal appearance, and narrowed distribution. The CSP-dP-NCs treated arthritic animals demonstrated the improved bodyweight and haematological parameters. The levels of thymus and spleen index and hind paw volume was decreased by the CSP-dP-NCs. The administration of CSP-dP-NCs to the arthritic rats also exhibited the decreased contents of IL-6, IL-10, IL-1β, TNF-α, MDA levels and increased the GSH level, CAT and SOD activities. The activities of ALP, ALT, and ASP also decreased in arthritic rats by the CSP-dP-NCs treatment.

Conclusion: Altogether, the findings of this study demonstrated the antiarthritic activity of formulated CSP-dP-NCs against FCA-induced arthritic rats via modulating oxidative stress and inflammatory parameters. Hence, it could be the effective drug for the arthritis treatment in the future.

1. Introduction

Arthritis is a progressive inflammatory disease that mainly affect the bone joints. The prolonged arthritis can result in socioeconomic burdens, poor life quality of patients, severe disability, and early mortality due to the deformity and destruction of joints (Quan et al., 2008). The incidence of arthritis in women population are likely 2–3 times higher than in men and new cases of arthritis is rapidly increasing around the world (Hunter et al., 2017). Nearly 3% of global population is affected by the arthritis. It causes severe physical distress and pain also puts patients at the risks of work disability as it arises in peoples with 30–40 years age group (Hoving et al., 2014). The early signs of arthritis progression is swelling around joints, heat, restricted movement, pain and decreased joint function and in developed stage displays the deformity and joint stiffness leading to bone injury and disability (Singh et al., 2015; Surai, 2006). During the pathogenesis of of osteoarthritis, both environmental and genetic causes plays a major roles, though the precise root cause of arthritis is not discovered yet (Hultqvist et al., 2006).

Arthritis has a close connections with inflammatory condition, as it developed by several immune cells and inflammatory regulators (Sengupta et al., 2011; Kamel et al., 2018). The crucial inflammatory cytokines that actively participates in the inflammatory signalings during arthritis development is interleukin (IL)-6, IL-1β, and TNF-α that primarily expressed in the bone joints during initial phases of inflammation (Hata et al., 2004). These mediators can aggravate the inflammation and development of development of osteoarthritis. TNF-α is one of the most imperative inflammatory cytokine responsible for increased synovial proliferation and augmented expressions of other inflammatory like IL-1β (Hegemann et al., 2003). These pathological changes eventually lead to the destruction of bones, cartilages, and joints, and even provoke disability. IL-6 and IL-1β are the vital players of arthritis development development. The augmented levels of IL-6 and IL-1β was found in the synovial membrane and fluids of arthritis joints (McInnes and Schett, 2007). During the developed stage, the increased level of IL-6 can be detected in the blood samples that proves its participation in the later stage of arthritis (Szekanecz et al., 2000). The inhibition of the cytokines production like TNF-α, IL-6, and NF-κB could diminish the inflammatory reactions during arthritis development (Aggarwal et al., 2013).

At present, there are no effective treatment options for arthritis. The current treatment approaches comprise medications like disease modifying antiarthritic drugs (DMARDs) and nonsteroidal anti-inflammatory drugs (NSAIDs), lifestyle changes, and physical therapies. The general medications applied for pain relief purpose and deferment of arthritis development comprises acetaminophen, indomethacin, leflunomide, methotrexate, corticosteroids, abatacept, and rituximab (Gaffo et al., 2006). Additionally, the combined administration of these drugs is a major approach for the arthritis treatment. Though NSAIDs and DMARDs ameliorates both inflammation, pain and arthritis, but these medications often experienced with increased adverse effects on patients like risks of cardiovascular and gastrointestinal problems, primarily because of the heavy doses and prolonged administrations (Sostres et al., 2010).

The usage of new drug delivery mechanisms may decrease the adverse effects of drugs and resolve the complications like stability and solubility of drug candidates with increased therapeutic potential, additionally assisting the patients to acceptance (Wang et al., 2021; Alvarez-Lorenzo et al., 2013). The controlled drug delivery technique has gained much attention in recent times to supply the drugs as required volume at targeted sites to gain the preferred results (Alemdar, 2016; Bahadoran et al., 2021; Li et al., 2019). The amalgamation of drug with the substrates with definite physical, chemical, and biological properties is an major strategy of controlled

drug supply (Vatanparast and Shariatinia, 2019; Rambhia and Ma, 2015). The nanomedicines have transformed pharmaceutical field for improved and targeted treatments for manifold ailments (Chen et al., 2021). The comparatively smaller size and improved surface area of nano-carriers permit selective supply of drugs to the targeted sites with less adverse effects on normal cells/tissues. Nano-carriers also improve the biological action of drugs via elevating their solubility (Chang et al., 2015).

Chitosan, a natural biopolymer is a promising candidate that extensively studied in drug delivery mechanisms due to its specific low cost, biodegradability, biocompatibility, and nontoxic natures (Kolawole et al., 2019; Shariatinia and Jalali, 2018). D-pinitol is a natural bioactive compound mostly found in the leaves of Sutherlandia frutescens (Negishi et al., 2015). D-pinitol showed several biological activities like antioxidant (Moreira et al., 2018), antidiabetic (Gao et al., 2015), anti-inflammatory (Singh et al., 2001), and anticancer (Sethi et al., 2008) properties. But the effectiveness of D-pinitol amalgamated nanocomposites on the inflammatory diseases like arthritis was not explored yet. Therefore, the current research work was focussed to formulate the chitosan-sodium alginate-polyethylene glycol-d-pinitol nanocomposites (CSP-dP-NCs) and assessed its therapeutic effects against the freund's complete adjuvant (FCA)-provoked arthritis in animals.

2. Materials and methods

2.1. Chemicals

D-pinitol, chitosan, polyethylene glycol, sodium alginate, and other reagents and chemicals were purchased from the Sigma-Chemicals, USA. All assay kits were attained from MyBiosource and Thermofisher, USA.

2.2. Synthesis of CSP-dP-NCs

For the preparation of CSP-dP-NCs, the D-pinitol was suspended in 20 ml of DMSO and added with the 0.1 % (wt/vol) of chitosan solution prepared in 200 ml of 1% acetate acid under continuous stirring until suspension was developed. After that, the suspension was ultrasonicated for reducing the nanoparticle droplets. For coating purpose, the prepared suspension, which consisting D-pinitol and chitosan was released into the polymer solution that containing sodium alginate and polyethylene glycol. After the completion of coating process, the formulated nanocomposites powder was obtained by dehydrating the final suspension by spray pyrolysis process, with the temperature 80–100 °C and airflow (5 L/min) (Lim et al., 2019).

3. Characterization of synthesized CSP-dP-NCs

3.1. UV–visible spectral analysis

To confirm the development of CSP-dP-NCs in the reaction solution, the UV–visible spectral study was performed with the help of Shimadzu-1700, Japan. The formation of CSP-dP-NCs were confirmed by the UV–vis spectral analysis. The absorbance of samples were measured at wavelength ranging from 400 to 1000 nm.

3.2. Photoluminescence spectroscopic analysis

The formulated of CSP-dP-NCs were examined by the photoluminescence spectroscopic study and the spectra results were taken at λexc = 405 nm using Roithner Laser Technik, Germany.

3.3. Ray diffraction (XRD) analysis

The synthesized CSP-dP-NCs were studied by using X-ray diffractometer (X'pert Pro PANalytical) system. The prepared samples were investigated at 45 mA and 40 kV voltage and scanned for 0.02–0.5 s. The obtained results were further analysed.

3.4. Fourier Transform-Infrared (FT-IR)

The functional groups exists on the surface of formulated CSP-dP-NCs were assessed by FT-IR study. In brief, the powdered sample was investigated by FT-IR instrument (Shimadzu-8400S, Japan). The FT-IR spectrum of fabricated CSP-dP-NCs were taken by potassium bromide (KBr) disc method. The FT-IR spectrum was studied by 4000–400 cm^{-1} ranges with the resolution at 4 cm^{-1} for 50 scans.

3.5. Scanning electron microscopic (SEM) and energy dispersive X-ray (EDX) analysis

The size, appearance, and components of fabricated CSP-dP-NCs were examined by SEM instrument equipped with EDX under normal atmospheric conditions. The fabricated CSP-dP-NCs were studied by SEM instrument (Carl Zeiss Ultra 55 FESEM). The prepared CSP-dP-NCs sample was located on the glass slide, uniformly dispersed, and dehydrated in vacuum. Lastly, the samples were studied by SEM machine under high vacuum at several magnifications.

3.6. Dynamic light scattering (DLS) assay

The average size and distribution patterns of synthesized CSP-dP-NCs were assessed by using DLS machine Zeta sizer (Malvern, USA).

3.7. Experimental animals

The 55 days aged Sprague-Dawley (SD) rats, weighing 240–270 g were chosen for this research study and animals were purchased from institutional animal house. Animals were housed in sanitized polypropylene cabins and preserved at well organized laboratory conditions with temperature 22–26 °C, air moisture 40–70 %, and 12-h light/dark series. Rats were given free access to rodent diet and pure drinking water. Before the initiation of experiments, all animals were acclimatized for a week in the laboratory to ensure the animal well being.

3.8. Treatment procedures

The acclimatized rats were randomly distributed into four individual groups with six rats in each. The group-I aided as normal control without any treatments and provided with regular rodent diet. Group-II are arthritis initiated animals through administering 0.1 ml of FCA by sub-cutaneous route to provoke the arthritis (Bendele, 2001). The group-III were arthritis-provoked animals supplemented with 10 mg/kg of formulated CSP-dP-NCs by oral route for 25 days. The group-IV rats were arthritis provoked and 30 mg/kg of CSP-dP-NCs supplemented animals. The initial and final bodyweight of each rats were taken and data were tabulated.

3.9. Hematological analysis

After the completion of experiments, all animals were anesthetized and sacrificed, then blood samples were drawn by *retro*-orbital method. The gathered blood samples were used to detect the hematological markers like red blood cells (RBCs), white blood cells (WBCs), and hemoglobin (Hb) by using automated hematological analyzer (Beckman Coulter, Brea, CA, USA).

3.10. Measurement of organ index

After the sacrification, the spleen and thymus organs were dissected out from control and treated animals and weighed precisely and data were tabulated to measure the organ index. The final data were depicted as mg/g.

3.11. Measurement of hind paw volume

The injected hind paw (right) volume of both control and treated animals were measured carefully from initiation and completion of experimental period (day 1–25). The variations in paw volume between treatment groups were assessed and data were tabulated.

3.12. Study of spleen cell proliferation

The excised spleen tissues from the experimental rats were cut into small pieces and squashed gently in an 5 ml of RPMI medium enriched with FBS (0.5 %). The spleen cell suspension were then filtered and centrifuged at 2000 rpm for 5 mins. After that, 5 ml of ACK buffer, which contains 8.29 g of ammonium chloride, 1 g of potassium bicarbonate, and 32.2 g of EDTA were mixed to the tissue suspension to remove the RBCs. Then the cells were placed on the growth medium at 1×10^6 cells/ml and sustained at 37 °C for 72 hrs in an 5 % CO_2 provided chamber. Afterward, 25 µl of MTT reagent and then 100 µl of DMSO was added to each well. Finally, the intensity of formed color were investigated at 495 nm and then spleen cell proliferation index was determined.

3.13. Assessment of liver function biomarkers

The enzymatic activities of liver function biomarker enzymes like alkaline phosphatase (ALP), alanine transaminase (ALT), and aspartate transaminase (AST) in the serum of normal control and treated animals were identified by using specific assay kits as per the guidelines specified by manufacturer (Biocompare, USA).

3.14. Quantification of oxidative stress and antioxidant biomarkers

The content of malondialdehyde (MDA), and antioxidant markers like superoxide dismutase (SOD) activity, catalase (CAT) activity, and glutathione (GSH) content in the control and treated animals were assessed by using assay kits by the guidelines specified by manufacturer (R&D Systems, Minneapolis, USA).

3.15. Quantification of pro-inflammatory marker levels

The inflammatory biomarkers like inerleukin-1β (IL-1β), IL-6, , IL-10, and TNF-α levels in the serum of experimental rats were assessed by using respective kits according to the guidelines of manufacturer (Mybiosource, USA).

3.16. Statistical analysis

The obtained results were assessed statistically with the help of GraphPad Prism software. The final data were illustrated as mean ± SD of triplicates measurements. The one-way ANOVA and Tukey post doc assay were performed to measure the variations between groups and $p < 0.05$ was set as significant.

4. Results

4.1. Characterization studies of synthesized CSP-dP-NCs

4.1.1. Uv–visible spectral analysis

The fabricated CSP-dP-NCs were examined by using UV–visible spectroscopic analysis for the confirmation. The absorbance synthesized CSP-dP-NCs were analysed at various wavelengths ranging from 400 to 1000 nm. As illustrated in the Fig. 1(A), the maximum peak was observed at 280 nm, which proves the existence of synthesized CSP-dP-NCs.

4.2. Photoluminescence analysis

Fig. 1(B) shows the photoluminescence spectrum of fabricated CSP-dP-NCs. The excitation of CSP-dP-NCs were found at 367 nm, 399 nm, 434 nm, and 478 nm, respectively that confirms the existence of CSP-dP-NCs. The peaks at 367 nm and 399 nm may resembles the free exciton recombination. The blue and blue-green emissions were observed at 434 nm and 478 nm and these peaks may attributes to interstitial oxygen vacancies.

4.3. XRD analysis

The fabricated CSP-dP-NCs were examined by using XRD purity and crystallinity and data were depicted in the Fig. 2 (A). The formulated CSP-dP-NCs demonstrated the various peaks located at (110), (002), (111), (−202), (020), (202), (−113), (−311), and (220), which denotes the face-centered

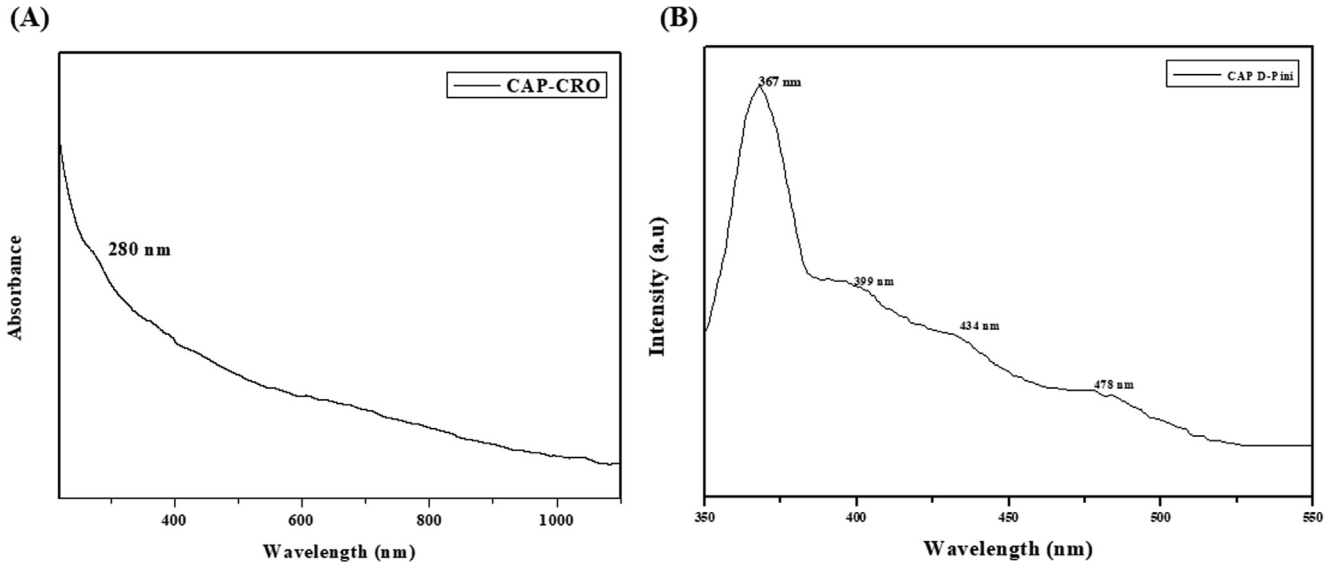

Fig. 1 UV–visible spectrum and photoluminescence analysis. (A): UV–Visible spectrum of synthesized CSP-dP-NCs. The maximum absorption peak was noted at 280 nm. (B): Photoluminescence spectrum of fabricated CSP-dP-NCs. The excitation of CSP-dP-NCs were found at 367 nm, 399 nm, 434 nm, and 478 nm, respectively.

tetragonal structural arrangements (Fig. 2A). The purity and crystallinity of the formulated CSP-dP-NCs were confirmed.

4.4. Ft-IR analysis

The frequencies of functional groups that exists in the surface of fabricated CSP-dP-NCs were identified by using FT-IR and the outcomes were illustrated in the Fig. 2(B). As depicted in the Fig. 2(B), the FT-IR spectrum of fabricated CSP-dP-NCs demonstrated several peaks at diverse frequencies. The peak found in 3402 indicates the band attributes to hydroxyl (O—H) stretching. The peak at 2930 cm^{-1} demonstrates the presence of H stretching. The several peaks at 1586 cm^{-1}, 1417 cm^{-1}, and 1019 cm^{-1} exhibits the bending vibrations of C—O and C—H bonds. The various peaks at 963 cm^{-1}, 619 cm^{-1}, and 503 cm^{-1} demonstrates the O—H bonds and nanocomposites.

4.5. SEM and EDX analysis

Fig. 3(A&B) depicts the SEM and EDX analyses of formulated CSP-dP-NCs. The SEM photographs of CSP-dP-NCs

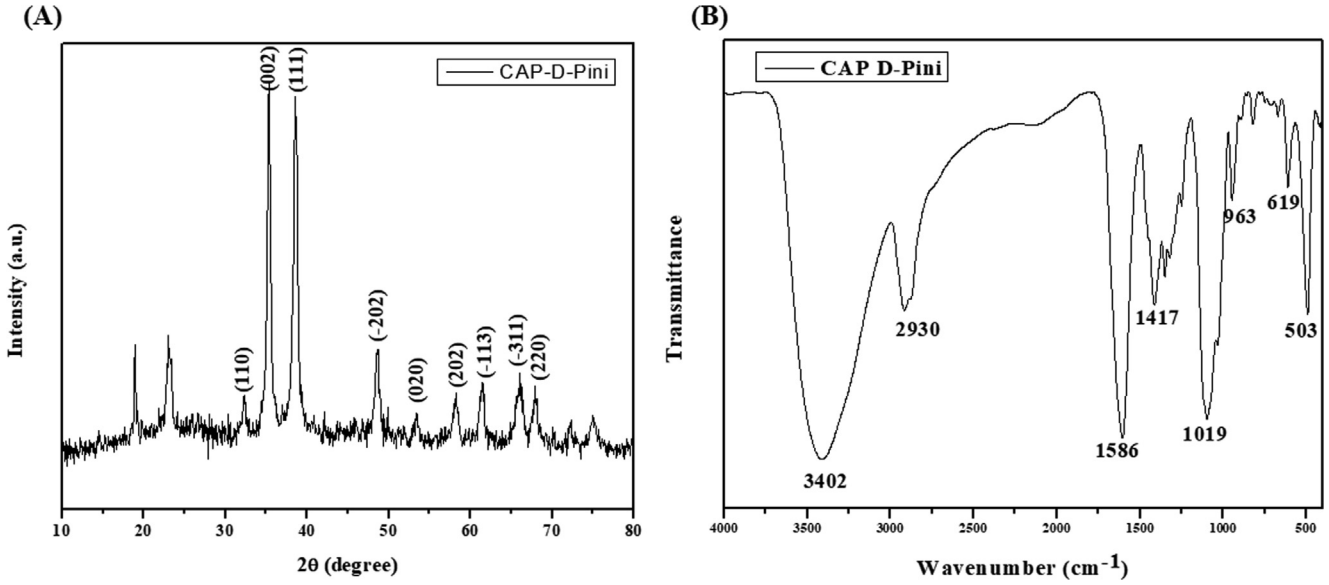

Fig. 2 XRD and FT-IR analysis of synthesized CSP-dP-NCs (A): XRD analysis of formulated CSP-dP-NCs showed the crystalline nature. (B): FT-IR spectrum of CSP-dP-NCs demonstrated the existence of O—H, H, C—O, C—H, O—H stretching, which is confirmed by various peaks.

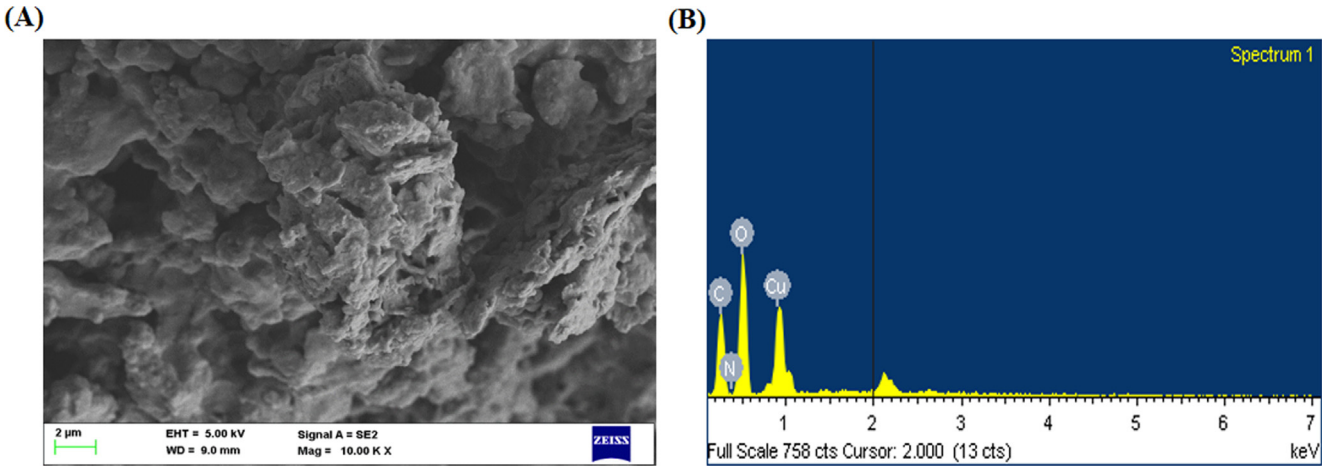

Fig. 3 SEM and EDX analysis of synthesized CSP-dP-NCs. (A): SEM analysis of fabricated CSP-dP-NCs exhibits the irregular and tetragonal appearance. (B): EDX analysis of synthesized CSP-dP-NCs revealed the presence carbon, nitrogen, copper and oxygen components.

revealed the agglomerated surface morphology with tetragonal appearance. The EDX study was done to identify the components present in the CSP-dP-NCs. The characteristic peaks of EDX analysis revealed the presence carbon, nitrogen, copper and oxygen demonstrated by pinitol.

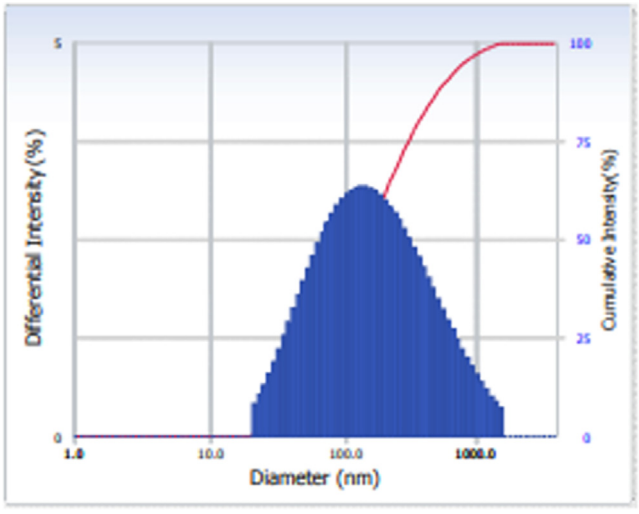

Fig. 4 DLS analysis of synthesized CSP-dP-NCs. The DLS analysis of synthesized CSP-dP-NCs revealed the distinctive peak with a size ranging from 180 nm with narrowed distribution.

4.6. DLS analysis

The size and distribution patterns of formulated CSP-dP-NCs were examined by DLS analysis and the data were displayed in the Fig. 4. The outcomes of DLS analysis revealed the distinctive peak with a size of ranging from 180 nm with narrowed distribution.

4.7. Effect of synthesized CSP-dP-NCs on the haematological parameters of FCA-induced arthritic animals

The effects of formulated CSP-dP-NCs on the haematological markers like RBCs, WBCs, and Hb in the FCA-provoked arthritis rats were assessed and data showed in the Table 1. The FCA-challenged arthritis animals demonstrated the marked reduction in both RBCs and Hb, whereas improved the WBCs level when compared with control. The treatment with 10 and 25 mg/kg of formulated CSP-dP-NCs displayed the substantial increment in both RBCs and Hb levels on the FCA-challenged arthritic animals (Table 1). The CSP-dP-NCs treatment also decreased the level of WBCs in the arthritis animals.

4.8. Effect of synthesized CSP-dP-NCs on the bodyweight and organ index on the FCA-induced arthritic animals

Fig. 5 exhibits the effects of fabricated CSP-dP-NCs on the bodyweight and organ index of arthritic animals. The FCA-

Table 1 Effect of synthesized CSP-dP-NCs on the haematological parameters of FCA-induced arthritic animals.

Groups	RBC ($\times 10^6$/µl)	WBC ($\times 10^3$/µl)	Hb (g/dl)
Group I	10.51	10.55	11.4
Group II	2.6$^{\#}$	19.22$^{\#}$	3.40$^{\#}$
Group III	4.72*	13.64*	8.61*
Group IV	7.4*	12.47*	10.08*

Values were depicted as mean ± SD of triplicate measurements. Significance was assessed by one-way ANOVA and Tukey's post hoc assay; '#' $p < 0.05$ when evaluated with control, '*' $p < 0.01$ when evaluated with FCA-challenged arthritic group. Note: Group I: Normal control rats, Group II: FCA-challenged arthritic rats, Group III: FCA-challenged arthritic rats treated with 10 mg/kg of CSP-dP-NCs, Group IV: FCA-challenged arthritic rats treated with 25 mg/kg of CSP-dP-NCs.

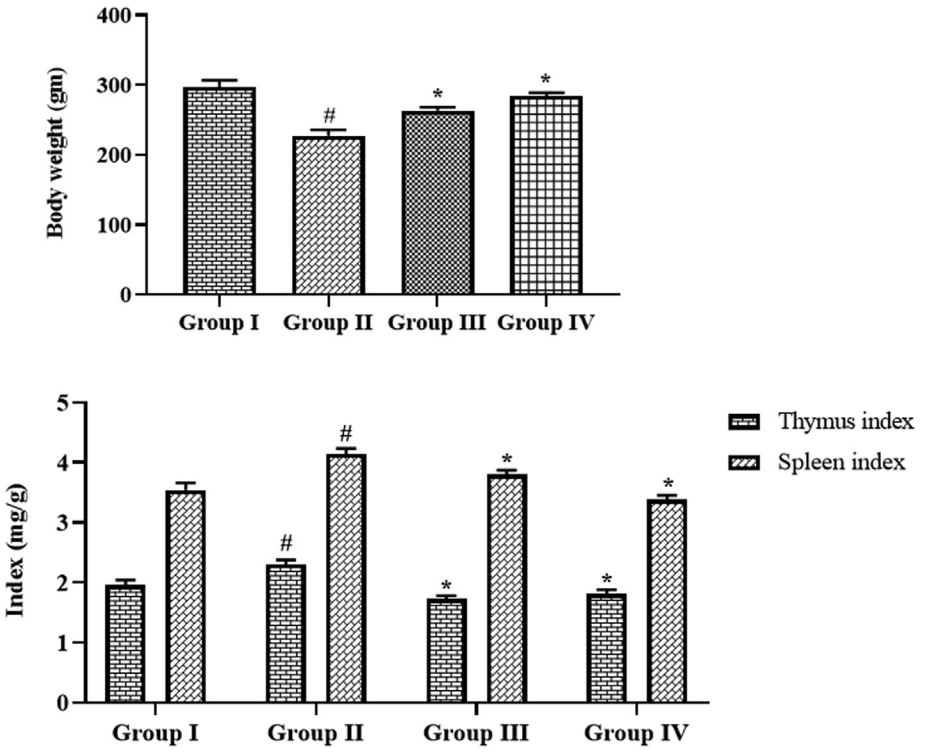

Fig. 5 Effect of synthesized CSP-dP-NCs on the bodyweight and organ index on the FCA-induced arthritic animals. Each bar depicts the mean ± SD of triplicate measurements. Significance was assessed by one-way ANOVA and Tukey's post hoc assay; '#' $p < 0.05$ when evaluated with control, '*' $p < 0.01$ when evaluated with FCA-challenged arthritic group. Note: Group I: Normal control rats, Group II: FCA-challenged arthritic rats, Group III: FCA-challenged arthritic rats treated with 10 mg/kg of CSP-dP-NCs, Group IV: FCA-challenged arthritic rats treated with 25 mg/kg of CSP-dP-NCs.

provoked arthritic animals demonstrated the decreased bodyweight when compared with control animals. The treatment with 10 and 25 mg/kg of synthesized CSP-dP-NCs effectively improved the bodyweight of arthritic rats. The arthritic rats also displayed the increased thymus and spleen weights when evaluated with control. Interestingly, the administration of 10 and 25 mg/kg of formulated CSP-dP-NCs decreased the thymus and spleen weights in the arthritic animals (Fig. 5).

4.9. Effect of synthesized CSP-dP-NCs on the hind paw volume of FCA-induced arthritic animals

The effects of formulated CSP-dP-NCs treatment on the hind paw volume of arthritic rats were examined at different time period (day 5–25) and data were depicted in the Fig. 6. The FCA-challenged arthritic animals demonstrated the marked increment in the hind paw volume, when related with control.

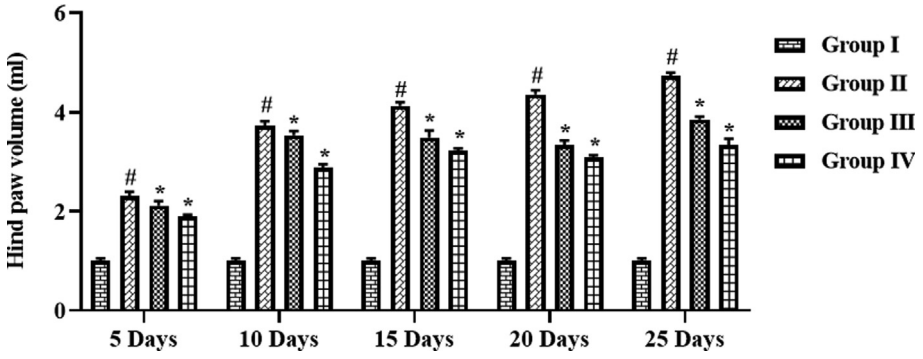

Fig. 6 Effect of synthesized CSP-dP-NCs on the hind paw volume of FCA-induced arthritic animals. Each bar depicts the mean ± SD of triplicate measurements. Significance was assessed by one-way ANOVA and Tukey's post hoc assay; '#' $p < 0.05$ when evaluated with control, '*' $p < 0.01$ when evaluated with FCA-challenged arthritic group. Note: Group I: Normal control rats, Group II: FCA-challenged arthritic rats, Group III: FCA-challenged arthritic rats treated with 10 mg/kg of CSP-dP-NCs, Group IV: FCA-challenged arthritic rats treated with 25 mg/kg of CSP-dP-NCs.

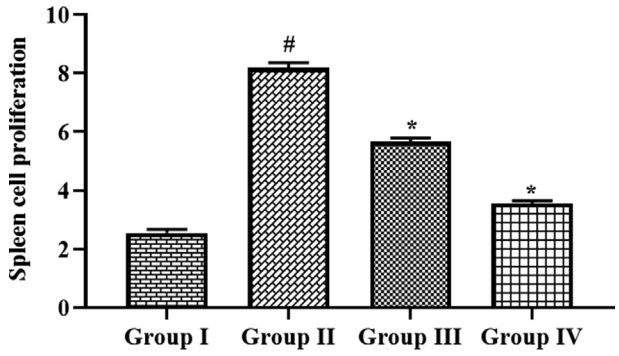

Fig. 7 Effect of synthesized CSP-dP-NCs on the spleen cell proliferation in the FCA-induced arthritic animals. Each bar depicts the mean ± SD of triplicate measurements. Significance was assessed by one-way ANOVA and Tukey's post hoc assay; '#' $p < 0.05$ when evaluated with control, '*' $p < 0.01$ when evaluated with FCA-challenged arthritic group. Note: Group I: Normal control rats, Group II: FCA-challenged arthritic rats, Group III: FCA-challenged arthritic rats treated with 10 mg/kg of CSP-dP-NCs, Group IV: FCA-challenged arthritic rats treated with 25 mg/kg of CSP-dP-NCs.

However, the treatment with 10 and 25 mg/kg of fabricated CSP-dP-NCs to the FCA-provoked arthritic animals demonstrated the considerable reduction in paw volume, when evaluated with FCA alone treated arthritic rats (Fig. 6). These findings confirmed the therapeutic effects of CSP-dP-NCs.

4.10. Effect of synthesized CSP-dP-NCs on the spleen cell proliferation in the FCA-induced arthritic animals

The effects of fabricated CSP-dP-NCs on the proliferation index of spleen cells from the FCA-challenged arthritic animals were assessed and findings were depicted in the Fig. 7. The spleen cells of FCA-provoked arthritic animals demonstrated the increased proliferation when compared with untreated control animal spleen cells. Nonetheless, the spleen cells from the 10 and 25 mg/kg of fabricated CSP-dP-NCs administered arthritic animals exhibited the decreased proliferation, when compared with FCA alone treated cells (Fig. 7). The 25 mg/kg of CSP-dP-NCs effectively decreased the spleen cell proliferation.

4.11. Effect of synthesized CSP-dP-NCs on the liver function marker enzymes in the FCA-induced arthritic animals

The activities of liver function biomarker enzymes like AST, ALP, and ALT in the serum of both control and experimental rats were assessed and findings were showed in the Fig. 8. The increased ALT, AST, and ALP activities were observed in the serum of FCA-challenged arthritic animals. These increments effectively reversed by the formulated CSP-dP-NCs treatment. The administration of 10 and 25 mg/kg of synthesized CSP-dP-NCs were substantially decreased the ALT, ALP, and AST activities in the serum of FCA-challenged arthritic animals (Fig. 8).

5. Effect of synthesized CSP-dP-NCs on the oxidative stress and antioxidant markers in the FCA-induced arthritic animals

Fig. 9 demonstrates the effects of CSP-dP-NCs treatment on the oxidative stress and antioxidant biomarker levels in the arthritic rats. The increased levels of MDA was observed in the FCA-provoked arthritic animals when compared with control. The treatment with the 10 and 25 mg/kg of formulated CSP-dP-NCs were showed the marked reduction on MDA level in the arthritic animals. The arthritic animals also exhibited the reduced GSH level, SOD and CAT activities when related with the control. Appreciably, the supplementation of 10 and 25 mg/kg of synthesized CSP-dP-NCs improved the GSH level, CAT and SOD activities in the FCA-treated arthritic animals (Fig. 9).

5.1. Effect of synthesized CSP-dP-NCs on the inflammatory cytokines level in the FCA-induced arthritic animals

The effects of fabricated CSP-dP-NCs treatment on the inflammatory cytokine levels in the FCA-challenged arthritic animals were assessed and data were showed in the Fig. 10. The increased levels of IL-6, IL-1β, and TNF-α were noted in the serum of FCA-challenged arthritic animals. However, the treatment with the 10 and 25 mg/kg of formulated CSP-dP-NCs demonstrated the appreciable reduction on the IL-6, IL-1β, and TNF-α in a serum of FCA-provoked arthritic rats. The arthritic animals also demonstrated the decreased level of IL-10 in the serum when compared with control. Nonetheless, the 10 and 25 mg/kg of formulated CSP-dP-NCs treatment improved the IL-10 level in the serum of arthritic animals (Fig. 10).

6. Discussion

Arthritis is a chronic inflammatory disease characterized by swelling, stiffness, pain, synovial hyperplasia, and bone destruction, which can lead to serious deformity and disability (Xu et al., 2016; Kyei et al., 2012). NSAIDs has analgesic effect in the early stage of arthritis, but they were often reported with insufficient efficacy and several side effects like renal, gastrointestinal, and cardiovascular risks (Mitragotri and Yoo, 2011; Rao and Knaus, 2008).

The synthetic DMARDs has specific anti-rheumatic effects but they can also bring several side effects like liver cirrhosis, hypersensitivity, retinopathy, allergy, interstitial pneumonitis, and myelo-suppression (von Vollenohower, 2009). As an effective alternative to conventional therapies, nanomedicines received much attention and possessed promising therapeutic solution for the arthritis treatment (Ashraf et al., 2021; Rubinstein and Weinberg, 2012). The site-specific targeted drug delivery of nano-medicines facilitates manifold applications like enhancement of therapeutic actions, protecting drugs from degradation, and lessening of side effects (Prasad et al., 2015; Yang et al., 2017). Nanomedicine has developed as a novel therapeutic approach to attain effective drug delivery to treat several diseases (Eskandari et al., 2020; Shi et al., 2017). In recent times, the formulation of nano-medicines for arthritis treatment was increased rapidly due to its potential to accumulate effectively in the inflammatory sites of arthritic

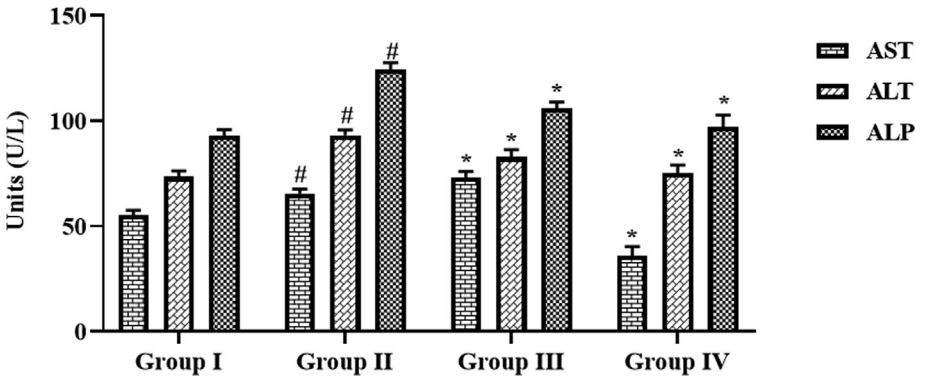

Fig. 8 Effect of synthesized CSP-dP-NCs on the liver function marker enzymes in the FCA-induced arthritic animals. Each bar depicts the mean ± SD of triplicate measurements. Significance was assessed by one-way ANOVA and Tukey's post hoc assay; '#' $p < 0.05$ when evaluated with control, '*' $p < 0.01$ when evaluated with FCA-challenged arthritic group. Note: Group I: Normal control rats, Group II: FCA-challenged arthritic rats, Group III: FCA-challenged arthritic rats treated with 10 mg/kg of CSP-dP-NCs, Group IV: FCA-challenged arthritic rats treated with 25 mg/kg of CSP-dP-NCs.

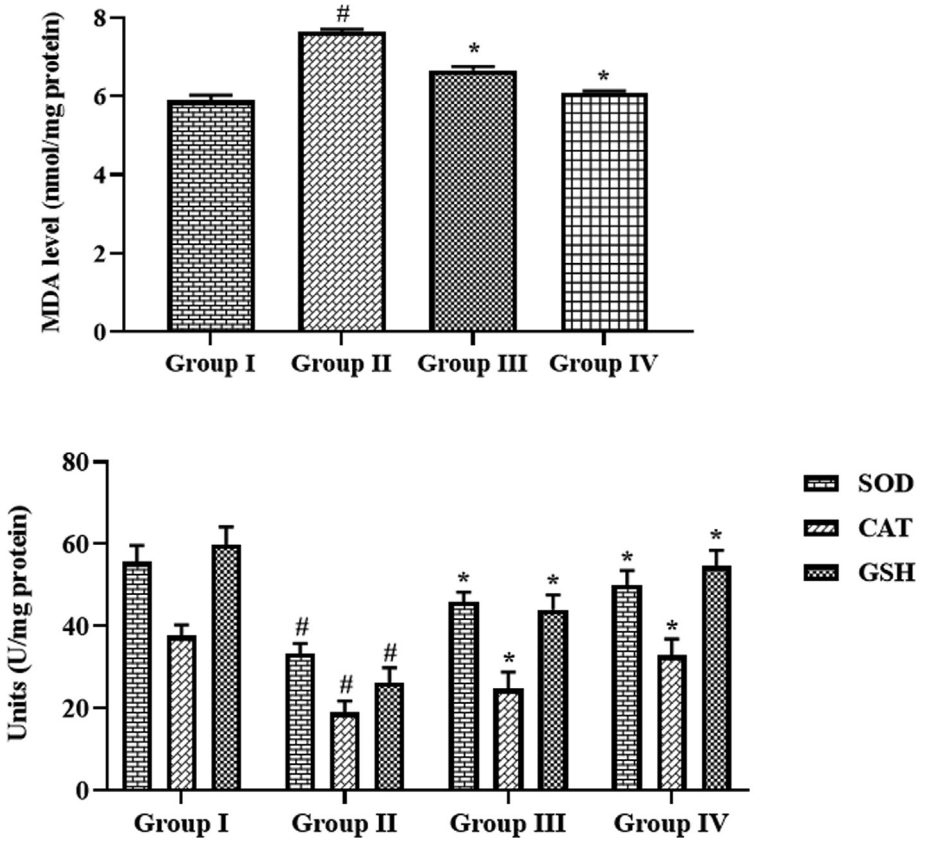

Fig. 9 Effect of synthesized CSP-dP-NCs on the oxidative stress and antioxidant markers in the FCA-induced arthritic animals. Each bar depicts the mean ± SD of triplicate measurements. Significance was assessed by one-way ANOVA and Tukey's post hoc assay; '#' $p < 0.05$ when evaluated with control, '*' $p < 0.01$ when evaluated with FCA-challenged arthritic group. Note: Group I: Normal control rats, Group II: FCA-challenged arthritic rats, Group III: FCA-challenged arthritic rats treated with 10 mg/kg of CSP-dP-NCs, Group IV: FCA-challenged arthritic rats treated with 25 mg/kg of CSP-dP-NCs.

joints. More than hundreds of various nanomedicine formulations were prepared and examined over the decades for numerous diseases and most of the being approved for clinical applications and many going through trials (Bobo et al., 2016). The pathological characteristics and mechanisms of the adjuvant-provoked arthritis is found similar to human arthritis, hence the adjuvant-stimulated arthritis model was extensively employed to study the antiarthritic roles of sample

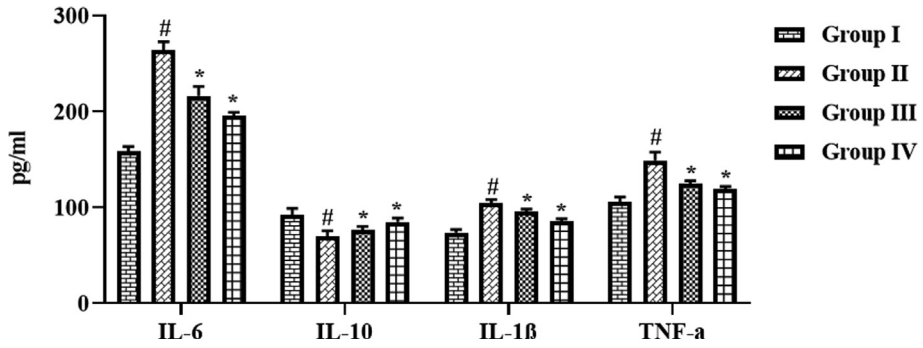

Fig. 10 Effect of synthesized CSP-dP-NCs on the inflammatory cytokines level in the FCA-induced arthritic animals. Each bar depicts the mean ± SD of triplicate measurements. Significance was assessed by one-way ANOVA and Tukey's post hoc assay; '#' $p < 0.05$ when evaluated with control, '*' $p < 0.01$ when evaluated with FCA-challenged arthritic group. Note: Group I: Normal control rats, Group II: FCA-challenged arthritic rats, Group III: FCA-challenged arthritic rats treated with 10 mg/kg of CSP-dP-NCs, Group IV: FCA-challenged arthritic rats treated with 25 mg/kg of CSP-dP-NCs.

drugs. Here, we formulated the CSP-dP-NCs and assessed its therapeutic potential against the adjuvant-stimulated arthritis in rats.

The changes in blood components provides basic information regarding inflammation due to arthritic condition and also shows the common physical condition of patients and indicate the disease severity. Arthritis develops as a severe inflammatory process that manifested by aneumia and elevated leukocytes. The increased leukocytes normally displays the progression of diseases. Leukocytes release several immunoregulatory and cytotoxic molecules and triggers oxidative stress through the increased generation of ROS. All these processes further drive into the development of arthritis (Cecchi et al., 2018). Several previous reports highlighted that the contents of Hb, RBC was found decreased and WBC were found elevated during arthritic condition. In arthritic condition, the RBC level was decreased and provokes anaemia due to the deformability of erythrocytes. The Hb is an another hematological marker found decreased in arthritic condition due to the destruction of premature RBCs and reduction of bone marrow erythropoietin (Patil et al., 2011; Premaratna et al., 2011). In similar manner, the decreased RBCs, Hb and increased WBCs were observed in the FCA-provoked arthritic rats. Interestingly, the supplementation of formulated CSP-dP-NCs were effectively increased the RBCs and Hb contents and also decreased the WBCs level in the arthritic animals. These findings demonstrates the therapeutic effects of fabricated CSP-dP-NCs.

The participation of inflammation in the arthritis pathogenesis is well described and several reports highlighted the roles of inflammatory cytokines in a development of arthritis. The increased levels of IL-6, IL-1β and TNF-α was already highlighted in several arthritis models (Alunno et al., 2017). These inflammatory mediators are facilitates to the destruction of bone joints and stimulate other cytokines production (Boissier et al., 2012). TNF-α is an imperative cytokine connected with inflammation and joint destruction by increased cytokine expression, angiogenesis promotion, inhibition of T-cells, and stimulation of pain (McInnes and Schett, 2011). The elevated expression of TNF-α triggers synovial inflammation and joint destruction (Choy and Panayi, 2001). TNF-α also stimulates synovial cells to generate more PGE2 and other inflammatory cytokines like IL-6 and IL-1β (Sun and Yokota, 2001). These inflammatory regulators aggravate the inflammatory reactions and facilitates to the synovial inflammation and joint injury. Consequently, the primary therapeutic targets in the arthritis treatment are pro-inflammatory cytokines and other inflammatory cells like synoviocytes and macrophages (Kinne et al., 2000). The inhibition of TNF-α and other inflammatory cytokines may facilitates to the prevention of arthritis (Weinblatt et al., 2003; Xu et al., 2011). Interestingly, here we found that the treatment with formulated CSP-dP-NCs were effectively depleted the contents of IL-6, IL-1β and TNF-α in the serum of FCA-challenged arthritic animals. The CSP-dP-NCs treatment also improved the IL-10 in the arthritic animals. These findings revealed the anti-inflammatory actions of formulated CSP-dP-NCs against the adjuvant-induced arthritis.

Oxidative stress is a crucial player of arthritis development and it arises due to the increased accumulation of ROS. The increased accumulation of oxidative stress markers like MDA was already reported in adjuvant-stimulated arthritis. During inflammatory condition, phagocytes accumulates in a bone joints and augment the levels of superoxide, hydroxyl, and hydrogen radicals. It was also described that the antioxidant biomarkers such as GSH, SOD, and CAT was found to be depleted in the arthritic conditions (Hitchon and El-Gabalawy, 2004). The augmented MDA level with reduced SOD activity often reported in arthritic condition (Tanwar et al., 2017). Similarly, the increased MDA, and depleted GSH, SOD and CAT activities were noted in the FCA-challenged arthritic animals. Interestingly, the treatment with fabricated CSP-dP-NCs effectively improved and antioxidants and decreased the MDA level in the arthritic animals. These findings suggested the antioxidant potential of fabricated CSP-dP-NCs. The enzymatic activities of ALT, AST, and ALP in a serum is the key indicator of liver function and disease condition. During inflammatory condition, ALP, ALT, and AST play a crucial functions in the generation of several chemical mediators like bradykinins. The augmented levels of these enzymes has been found in bone and liver that results in localized bone loss (Xu et al., 2017). Here, we found that the

FCA-challenged arthritic animals demonstrated the increased activities of ALT, AST, and ALP in the serum. But, the treatment with the formulated CSP-dP-NCs appreciably decreased the ALT, AST, and ALP enzyme activities in the arthritic rats. In overall, these findings suggested the therapeutic benefits of fabricated CSP-dP-NCs against the FCA-challenged arthritis in rats.

7. Conclusion

In conclusion, our findings confirmed the anti-inflammatory and anti-arthritic effects of fabricated CSP-dP-NCs against the FCA-provoked arthritis in rats. The treatment with CSP-dP-NCs effectively decreased the organ index, paw volume, and haematological parameters in the arthritic animals. The CSP-dP-NCs administration reduced the liver marker enzymes, pro-inflammatory cytokines level, and improved the antioxidants in the FCA-provoked arthritic rats. These findings recommended that fabricated CSP-dP-NCs could be a talented antiarthritic agent for the treatment of arthritis in the future.

Declaration of Competing Interest

The authors declare that they have no known competing financial interests or personal relationships that could have appeared to influence the work reported in this paper.

Acknowledgments

The authors would also like to extend their sincere appreciation to the Deanship of Scientific Research at King Saud University for its funding of this research through the Research Group Number (RG-1435-081).

References

Aggarwal, B.B., Gupta, S.C., Sung, B., 2013. Curcumin: an orally bioavailable blocker of TNF and other pro-inflammatory biomarkers. Br. J. Pharmacol. 169, 1672–1692.

Alemdar, N., 2016. Fabrication of a novel bone ash-reinforced gelatin/alginate/hyaluronic acid composite film for controlled drug delivery. Carbohydr. Polym. 151, 1019–1026.

Alunno, A., Carubbi, F., Giacomelli, R., Gerli, R., 2017. Cytokines in the pathogenesis of rheumatoid arthritis: new players and therapeutic targets. BMC Rheumatol. 1, 3.

Alvarez-Lorenzo, C., Blanco-Fernandez, B., Puga, A.M., Concheiro, A., 2013. Crosslinked ionic polysaccharides for stimuli-sensitive drug delivery. Adv. Drug Deliv. Rev. 65, 1148–1171.

Ashraf, M.A., Li, C., Zhang, D., Zhao, L., Fakhri, A., 2021. Fabrication of silver phosphate-ilmenite nanocomposites supported on glycol chitosan for visible light-driven degradation, and antimicrobial activities. Int. J. Biol. Macromol. 169, 436–442.

Bahadoran, A., Liu, Q., Masudy-Panah, S., De Lile, J.R., Ramakrishna, S., Fakhri, A., Gupta, V.K., 2021. Assessment of silver doped cobalt titanate supported on chitosan-amylopectin nanocomposites in the photocatalysis performance under sunlight irradiation, and antimicrobial activity. Surf. Interfaces 25, 101191.

Bendele, A., 2001. Animal models of rheumatoid arthritis. J. Musculoskelet. Neuronal Interact. 1, 377–385.

Bobo, D., Robinson, K.J., Islam, J., Thurecht, K.J., Corrie, S.R., 2016. Nanoparticle-based medicines: a review of FDA-approved materials and clinical trials to date. Pharm. Res. 33, 2373–2387.

Boissier, M.-C., Semerano, L., Challal, S., Saidenberg-Kermanac'h N, Falgarone G,, 2012. Rheumatoid arthritis: from autoimmunity to synovitis and joint destruction. J. Autoimmun. 39, 222–228.

Cecchi, I., Arias de la Rosa, I., Menegatti, E., Roccatello, D., Collantes-Estevez, E., Lopez-Pedrera, C., Barbarroja, N., 2018. neutrophils: novel key players in rheumatoid arthritis. Current and future therapeutic targets. Autoimmun. Rev. 17, 1138–1149.

Chang, E.H., Harford, J.B., Eaton, M.A., et al, 2015. Nanomedicine: past, present and future – a global perspective. Biochem. Biophys. Res. Commun. 468, 511–517.

Chen, Y., Cheng, H., Wang, W., Jin, Z., Liu, Q., Yang, H., Cao, Y., Li, W., Fakhri, A., Gupta, V.K., 2021. Preparation of carbon dots-hematite quantum dots-loaded hydroxypropyl cellulose-chitosan nanocomposites for drug delivery, sunlight catalytic and antimicrobial application. J. Photochem. Photobiol., B 219, 112201.

Choy, E.H., Panayi, G.S., 2001. Cytokine pathways and joint inflammation in rheumatoid arthritis. N. Engl. J. Med. 344, 907–916.

Eskandari, L., Andalib, F., Fakhri, A., Jabarabadi, M.K., Gupta, V. K., 2020. Facile colorimetric detection of Hg (II), photocatalytic and antibacterial efficiency based on silver-manganese disulfide/polyvinyl alcohol-chitosan nanocomposites. Int. J. Biol. Macromol. 164, 4138–4145.

Gaffo, A., Saag, K.G., Curtis, J.R., 2006. Treatment of rheumatoid arthritis. Am. J. Health Syst. Pharm. 63, 2451–2465.

Gao, Y., Zhang, M., Wu, T., Xu, M., Cai, H., Zhang, Z., 2015. Effects of D-Pinitol on insulin resistance through the PI3K/Akt signaling pathway in type 2 diabetes mellitus rats. J. Agric. Food Chem. 63 (26), 6019–6026.

Hata, H., Sakaguchi, N., Yoshitomi, H., Iwakura, Y., Sekikawa, K., Azuma, Y., Kanai, C., Moriizumi, E., Nomura, T., Nakamura, T., Sakaguchi, S., 2004. Distinct contribution of IL-6, TNF-alpha, IL-1, and IL-10 to T cell-mediated spontaneous autoimmune arthritis in mice. J Clin Invest. 114, 582–588.

Hegemann, N., Wondimu, A., Ullrich, K., Schmidt, M.F., 2003. Synovial mmp-3 and timp-1 levels and their correlation with cytokine expression in canine rheumatoid arthritis. Vet. Immunol. Immunopathol. 91, 199–204.

Hitchon, C.A., El-Gabalawy, H.S., 2004. Oxidation in rheumatoid arthritis. Arthritis Res. Ther. 6, 1–14.

Hoving, J.L., Lacaille, D., Urquhart, D.M., Hannu, T.J., Sluiter, J.K., Frings-Dresen, M.H.W., 2014. Non-pharmacological interventions for preventing job loss in workers with inflammatory arthritis. Cochrane Database Syst. Rev:CD010208.

Hultqvist, M., Olofsson, P., Gelderman, K.A., Holmberg, J., Holmdahl, R., 2006. A new arthritis therapy with oxidative burst inducers. PLoS Med. 3, e348.

Hunter, T.M., Boytsov, N.N., Zhang, X., Schroeder, K., Michaud, K., Araujo, A.B., 2017. Prevalence of rheumatoid arthritis in the United States adult population in healthcare claims databases, 2004–2014. Rheumatol. Intern. 37, 1551–1557.

Kamel, K.M., Gad, A.M., Mansour, S.M., et al, 2018. Novel anti-arthritic mechanisms of polydatin in complete Freund's adjuvant-induced arthritis in rats: involvement of IL-6, STAT-3, IL-17, and NF-rB. Inflammation 41, 1974–1986.

Kinne, R.W., Brauer, R., Stuhlmuller, B., Palombo-Kinne, E., Burmester, G.R., 2000. Macrophages in rheumatoid arthritis. Arthritis Res. 2 (3), 189–202.

Kolawole, O.M., Lau, W.M., Khutoryanskiy, V.V., 2019. Synthesis and evaluation of boronated chitosan as a mucoadhesive polymer for intravesical drug delivery. J. Pharm. Sci. 108, 3046–3053.

Kyei, S., Koffuor, G.A., Boampong, J.N., 2012. Antiarthritic effect of aqueous and ethanolic leaf extracts of pistia stratiotes in adjuvant-induced arthritis in sprague-dawley rats. J. Exp. Pharmacol. 4, 41–51.

Li, C., Wang, J., Wang, Y., Gao, H., Wei, G., Huang, Y., Yu, H., Gan, Y., Wang, Y., Mei, L., Chen, H., Hu, H., Zhang, Z., Jin, Y., 2019. Recent progress in drug delivery. Acta Pharm. Sin. B 9, 1145–1162.

Lim, H.R., Jung, S.J., Hwang, T.Y., Lee, J., Kim, K.H., Cho, H.B., et al, 2019. Electromagnetic wave absorption properties of Fe/MgO

composites synthesized by a simple ultrasonic spray pyrolysis method. Appl. Surf. Sci. 473, 1009–1013.
McInnes, I.B., Schett, G., 2007. Cytokines in the pathogenesis of rheumatoid arthritis. Nat. Rev. Immunol. 7, 429–442.
McInnes, I.B., Schett, G., 2011. The pathogenesis of rheumatoid arthritis. N. Engl. J. Med. 365, 2205–2219.
Mitragotri, S., Yoo, J.-W., 2011. Designing micro-and nano-particles for treating rheumatoid arthritis. Arch. Pharmacal Res. 34, 1887–1897.
Moreira, L.N., Silva, J.F., Silva, G.C., Lemos, V.S., Cortes, S.F., 2018. Activation of eNOS by Dpinitol induces an endothelium-dependent vasodilatation in mouse mesenteric artery. Front. Pharmacol. 9, 1–9.
Negishi, O., Mun'Im, A., Negishi, Y., 2015. Content of methylated inositols in familiar edible plants. J. Agric. Food Chem. 63 (10), 2683–2688.
Patil, C.R., Rambhade, A.D., Jadhav, R.B., et al, 2011. Modulation of arthritis in rats by Toxicodendron pubescens and its homeopathic dilutions. Homeopathy 100, 131–137.
Prasad, L.K., O'Mary, H., Cui, Z., 2015. Nanomedicine delivers promising treatments for rheumatoid arthritis. Nanomedicine 10, 2063–2074.
Premaratna, R., Halambarachchige, L.P., Nanayakkara, D.M., et al, 2011. Evidence of acute rickettsioses among patients presumed to have chikungunya fever during the chikungunya outbreak in Sri Lanka. Int. J. Infect. Dis. 15, e871–e873.
Quan, L.-D., Thiele, G.M., Tian, J., Wang, D., 2008. The development of novel therapies for rheumatoid arthritis. Exp. Opin. Thera. Pat. 18, 723–738.
Rambhia, K.J., Ma, P.X., 2015. Controlled drug release for tissue engineering. J. Control. Release 219, 119–128.
Rao, P., Knaus, E.E., 2008. Evolution of nonsteroidal anti-inflammatory drugs (NSAIDs): Cyclooxygenase (COX) inhibition and beyond. J. Pharm. Pharm. Sci. 11, 81–110.
Rubinstein, I., Weinberg, G.L., 2012. Nanomedicines for chronic non-infectious arthritis: the clinician's perspective. Nanomed. Nanotechnol. Biol. Med. 8, S77–S82.
Sengupta, K., Kolla, J.N., Krishnaraju, A.V., et al, 2011. Cellular and molecular mechanisms of anti-inflammatory effect of Aflapin: a novel Boswellia serrata extract. Mol. Cell. Biochem. 354, 189–197.
Sethi, G., Ahn, K.S., Sung, B., Aggarwal, B.B., 2008. Pinitol targets nuclear factor-κB activation pathway leading to inhibition of gene products associated with proliferation, apoptosis, invasion, and angiogenesis. Mol. Cancer Ther. 7 (6), 1604–1614.
Shariatinia, Z., Jalali, A.M., 2018. Chitosan-based hydrogels: preparation, properties and applications. Int. J. Biol. Macromol. 115, 194–220.
Shi, J., Kantoff, P.W., Wooster, R., Farokhzad, O.C., 2017. Cancer nanomedicine: progress, challenges and opportunities. Nat. Rev. Cancer 17 (1), 20–37.
Singh, S., Kumar, R., Jain, H., Gupta, Y.K., 2015. Anti-inflammatory and antiarthritic activity of UNIM-301 (a polyherbal unani formulation) in wistar rats. Pharmac. Res. 7 (2), 188–192.
Singh, R.K., Pandey, B.L., Tripathi, M., Pandey, V.B., 2001. Anti-inflammatory effect of (+)-pinitol. Fitoterapia 72, 168–170.
Sostres, C., Gargallo, C.J., Arroyo, M.T., Lanas, A., 2010. Adverse effects of non-steroidal anti-inflammatory drugs (NSAIDs, aspirin and coxibs) on upper gastrointestinal tract. Best Pract. Res. Clin. Gastroenterol. 24, 121–132.
Sun, H.B., Yokota, H., 2001. Altered mrna level of matrix metalloproteinase-13 in mh7a synovial cells under mechanical loading and unloading. Bone 28, 399–403.
Surai, P.F., 2006. Selenium in Nutrition and Health, vol. 974. Nottingham, UK: Nottingham University Press.
Szekanecz, Z., Halloran, M.M., Volin, M.V., Woods, J.M., Kenneth, Strieter R.M., Haines, G., Kunkel, S.L., Burdick, M.D., Koch, A. E., 2000. Temporal expression of inflammatory cytokines and chemokines in rat adjuvant-induced arthritis. Arthritis Rheum. 43, 1266–1277.
Tanwar, A., Chawla, R., Ansari, M.M., Neha, Thakur, P., Chakotiya, A.S., Goel, R., Ojha, H., Asif, M., Basu, M., et al, 2017. In vivo anti-arthritic efficacy of Camellia sinensis (L.) in collagen induced arthritis model. Biomed. Pharmacother. 87, 92–101.
Vatanparast, M., Shariatinia, Z., 2019. Hexagonal boron nitride nanosheet as novel drug delivery systemfor anticancer drugs: insights fromDFT calculations andmolecular dynamics simulations. J. Mol. Graph. Model. 89, 50–59.
von Vollenohower, R., 2009. Treatment of rheumatoid arthritis: state of the art. Nat. Rev. Rheumatol. 5, 531–541.
Wang, J., Sun, J., Huang, J., Fakhri, A., Gupta, V.K., 2021. Synthesis and its characterization of silver sulfide/nickel titanate/chitosan nanocomposites for photocatalysis and water splitting under visible light, and antibacterial studies. Mater. Chem. Phys. 272, 124990.
Weinblatt, M.E., Keystone, E.C., Furst, D.E., Moreland, L.W., Weisman, M.H., Birbara, C.A., Teoh, L.A., Fischkoff, S.A., Chartash, E.K., 2003. Adalimumab, a fully human anti-tumor necrosis factor alpha monoclonal antibody, for the treatment of rheumatoid arthritis in patients taking concomitant methotrexate: the ARMADA trial. Arthritis Rheum. 48, 35–45.
Xu, J., Itoh, Y., Hayashi, H., Takii, T., Miyazawa, K., Onozaki, K., 2011. Dihydrotestosterone inhibits interleukin-1alpha or tumor necrosis factor alpha-induced proinflammatory cytokine production via androgen receptor-dependent inhibition of nuclear factor-kappab activation in rheumatoid fibroblast-like synovial cell line. Biol. Pharm. Bull. 34, 1724–1730.
Xu, Q., Zhou, Y., Zhang, R., Sun, Z., Cheng, L., 2017. Antiarthritic activity of qi-wu rheumatism granule (a Chinese herbal compound) on complete freund's adjuvant-induced arthritis in rats. Evid. Complement. Altern. Med., 1–13
Xu, W., Huang, M., Zhang, Y., Li, H., Zheng, H., Yu, L., Chu, K., 2016. Extracts of Bauhinia championii (benth.) benth. Inhibit nf-<kappa>b-signaling in a rat model of collagen-induced arthritis and primary synovial cells. J. Ethnopharmacol. 185, 140–146.
Yang, M., Feng, X., Ding, J., Chang, F., Chen, X., 2017. Nanotherapeutics relieve rheumatoid arthritis. J. Control. Release 252, 108–124.